ISSN 0016-7029, Geochemistry International, 2020, Vol. 58, No. 2, pp. 189–199. © Pleiades Publishing, Ltd., 2020.
Russian Text © The Author(s), 2020, published in Geokhimiya, 2020, Vol. 65, No. 2, pp. 153–164.

Natural Magnesium Hydrous Orthophosphates Bobierrite and Kovdorskite: FTIR, Raman, Thermal, and Thermochemical Study

L. P. Ogorodova[a, *], Yu. D. Gritsenko[a, b], M. F. Vigasina[a], D. A. Kosova[c], L. V. Melchakova[a], and A. D. Fomina [a]

[a] *Geological Faculty, Moscow State University, Moscow, 119991 Russia*
[b] *Fersman Mineralogical Museum, Russian Academy of Sciences, Moscow, 119962 Russia*
[c] *Chemical Faculty, Moscow State University, Moscow, 119991 Russia*
**e-mail: logor@geol.msu.ru*

Received October 22, 2018; revised February 1, 2019; accepted February 4, 2019

Abstract—A physicochemical study of natural hydrous magnesium orthophosphates bobierrite $Mg_3[PO_4]_2 \cdot 8H_2O$ and kovdorskite $Mg_2[PO_4](OH) \cdot 3H_2O$ from the Kovdor carbonatite massif, Kola Peninsula, Russia, was carried out using X-ray diffraction, infrared spectroscopy, Raman spectroscopy, and thermal analysis. The enthalpies of dehydration of the minerals were measured using a NETZSCH DSC 204 F1 differential scanning calorimeter, the enthalpies of formation from the elements for bobierrite (–6167 ± 16 kJ/mol) and kovdorskite (–3251 ± 10 kJ/mol) were determined by high-temperature melt solution calorimetry on a Setaram high-temperature heat-flux Tian–Calvet microcalorimeter. The values of their standard entropies and Gibbs energies of formation are estimated.

Keywords: FTIR, Raman, thermal analysis, thermochemistry, enthalpy of formation, enthalpy of dehydration, bobierrite, kovdorskite

DOI: 10.1134/S0016702920020093

INTRODUCTION

Bobierrite $Mg_3[PO_4]_2 \cdot 8H_2O$ is a natural hydrous Mg phosphate belonging to the vivianite group. It occurs as colorless, yellow, white, and pale blue wedge-shaped split crystals, rosettes, fan-shaped aggregates, and spherulites, which line (together with collinsite, kovdorskite, and other rare phosphates) the walls of cavities in dolomite carbonatites among apatite ores and phoscorites, and as an alteration product of the phoscorites and apatite-group minerals. The crystal structure of bobierrite consists of single $[MgO_2(H_2O)_4]$ and doubled (sharing edges) $[Mg_2O_6(H_2O)_4]$ octahedrons connected with one another through PO_4^{3-} tetrahedrons to form layers parallel to (010). The neighboring layers are linked by the hydrogen bonds of water molecules (Takagi et al., 1986). Bobierrite crystallizes in the monoclinic system, space group $C2/c$.

Kovdorskite is a relatively rare hydrous Mg phosphate, whose formula is $Mg_2[PO_4](OH) \cdot 3H_2O$. This mineral sometimes contains small amounts of Fe and Mn. It was first found in 1969 in dolomite carbonatite of the Kovdor iron deposit in the Kola Peninsula, in cavities with dolomite, magnetite, hydrotalcite, manasseite, pyrite, bobierrite, and collinsite (Kapustin et al., 1980). The structure of kovdorskite is made up of clusters of four Mg octahedrons that share edges and one PO_4 tetrahedron (Ovchinnikov et al., 1980). Oxygen atoms occur in the apexes shared by Mg octahedrons and PO_4 tetrahedron, OH groups occur in apexes shared by three Mg octahedrons, and H_2O molecules occupy the other apexes of Mg octahedrons and apexes shared by two Mg octahedrons. The clusters occur in layers parallel to (001) in structural voids and define a pseudohexagonal motif. The layers are connected through $[PO_4]^{3-}$ tetrahedrons. Kovdorskite crystallizes in the monoclinic system, space group $P2(1)/a$. In contrast to bobierrite, kovdorskite contains not only crystal-hydrate H_2O molecules but also structural OH groups.

Kovdorskite and bobierrite are formed, together with other Mg and Ca carbonates and phosphates, during the late hydrothermal transformations of dolomite carbonatites and apatite–magnetite phoscorites, likely at temperatures no higher than 300°C (Ponomareva and Krasnova, 1990).

The structure of kovdorskite was studied and its unit-cell parameters were determined in (Kapustin et al., 1980; Ovchinnikov et al., 1980; Ponomareva and

Krasnova, 1990; Morrison et al., 2012), and bobierrite was studied in (Frazier et al., 1963; Kanazawa et al., 1979; Takagi et al., 1986; Liferovich et al., 1999). The minerals were studied by Raman and IR spectroscopy (Ponomareva and Krasnova, 1990; Liferovich et al., 1999; Frost et al., 2002; Morrison et al., 2012; Frost et al., 2013), and their thermal behavior was discussed in (Manly, 1950; Kapustin et al., 1980; Liferovich et al., 1999; Frost et al., 2013).

Data on thermodynamic properties of these minerals are limited to information on the Gibbs free energy of formation of bobierrite, and we are aware only of a single paper (Duff, 191) in which the value of $\Delta_f G^0$(298.15 K) was determined by studying the dissolution of Mg hydroorthophosphate newberyite $MgHPO_4 \cdot 3H_2O$. Data in (Vieillard and Tardy, 1984; La Iglesia, 2009) were acquired using various estimation techniques.

Our research involved a comprehensive physicochemical and thermochemical studies of kovdorskite and bobierrite by Calvet microcalorimetry and differential scanning calorimetry.

METHODS

This study was carried out with bobierrite and kovdorskite samples from the Kovdor carbonatite massif in the Kola Peninsula, Russia. These samples were made available for us by the Fersman Mineralogical Museum, Russian Academy of Sciences (bobierrite and kovdorskite sample nos. FN288 and FN287, respectively). The bobierrite sample consisted of single colorless transparent flattened crystals and radiating aggregates up to 2 cm across. The kovdorskite sample was an aggregate of colorless transparent flattened crystals 0.5–1.5 cm long, which were taken from radiating rosettes of this mineral hosted in magnetite–dolomite carbonatite.

The *chemical composition* of the minerals was analyzed on a Camebax-microbeam (France) microprobe equipped with an Si(Li) EDS detector and INCA Energy Oxford analytical system. The operation conditions were 20 kV accelerating voltage and 30 nA beam current.

The *X-ray diffraction identification* of the minerals was made in a STOE-STADI MP (Germany) X-ray powder diffractometer with a curved Ge(III) monochromator that ensured highly monochromatic Ca$K\alpha_1$ radiation (λ = 0.178897 Å). The data were acquired by successively covering scanning regions, using a position-sensitive linear detector (2Θ = 5°, channel width 0.02°).

The *Raman spectroscopic study* was conducted on an EnSpector R 532 (Russia) Raman microscope. The wavelength of the laser radiation was 532 nm, the laser output was approximately 16 mW, the holographic dispersion grating had 1800 lines/mm, the spectral resolution was 6 cm^{-1}, and the diameter of the focal spot varied from 1 to 2.5 μm at 40× magnification. The spectra were acquired within the region of 100 to 4000 cm^{-1}, using randomly oriented samples, at a counting time of 1 s and averaging over 50–100 positions.

The *IR spectroscopic study* was carried out on a FSM-1201 (LOMO, Russia) FTIR spectrometer within the range of 400 to 4000 cm^{-1}, with the frequencies determined accurate to ± 1 cm^{-1} in transmission mode in air at room temperature, using samples prepared in the form of suspensions in paraffinic oil.

The *thermal behavior* of the minerals up to 1200 K was studied on NETZSCH TG 209 F1 thermogravimetric analyzer in air flow (40 mL min^{-1}), at a heating rate of 10 K min^{-1}. The instrument was calibrated on the melting points of standard reference compounds (Ag, Al, Bi, and Sn 99.999% purity). The systematic inaccuracy of the weight measurements was no higher than 0.1%. The samples were weighed before the measurements on A&D GH-202 analytical scale balance accurate to 2×10^{-5} g. The masses of the samples were 5.38 mg for kovdorskite and 12.36 mg for bobierrite.

Thermochemical studies. The enthalpies of formation of the natural Mg phosphates were determined in a Setaram (France) Tian–Calvet microcalorimeter by dissolving in $2PbO \cdot B_2O_3$ melt. The samples 1.3–8.3 ($\pm 2 \times 10^{-3}$) mg were dropped from room temperature into solvent melt in a calorimeter at T = 973 K. The measured total heat involved the enthalpy of the mineral and its dissolution enthalpy [H^0(973 K) − H^0(298.15 K) + $\Delta_{dissol}H^0$(973 K)] (Kiseleva and Ogorodova, 1983). In six to eight experiments with melt portions of 30–35 g, the solute/solvent ratio approached that of an infinitely diluted solution, and the mixing enthalpy thus is infinitely close to zero. The calorimeter was calibrated by dropping a standard compound (platinum), with needed data on its [H^0(973 K) − H^0(298.15 K)] borrowed from (Robie and Hemingway, 1995).

The enthalpies of dehydration of the hydrous phosphates were measured on a NETZSCH DSC 204 F1 differential scanning calorimeter in a flow if high-purity nitrogen (40 mL min^{-1}) at a heating rate of 10 K min^{-1}. The instrument was calibrated for temperature and heat flux in compliance with recommendations of the ASTM E967 and ASTM E2253 standards. The standards were high-purity (99.999%) compounds whose parameters of phase transitions were determined highly accurately: cyclohexane C_6H_{12}, Hg, Ga, benzoic acid C_6H_5COOH, KNO_3, In, Sn, Bi, Pb, CsCl, and Zn. The systematic inaccuracies of the calibration curves were 0.1°C and 5% heat. The measurements were carried out in standard aluminum containers with punctured lids. The DSC curves thus acquired were processed with the NETZSCH Proteus Thermal Analysis software. The masses of the compounds were 4–6 mg.

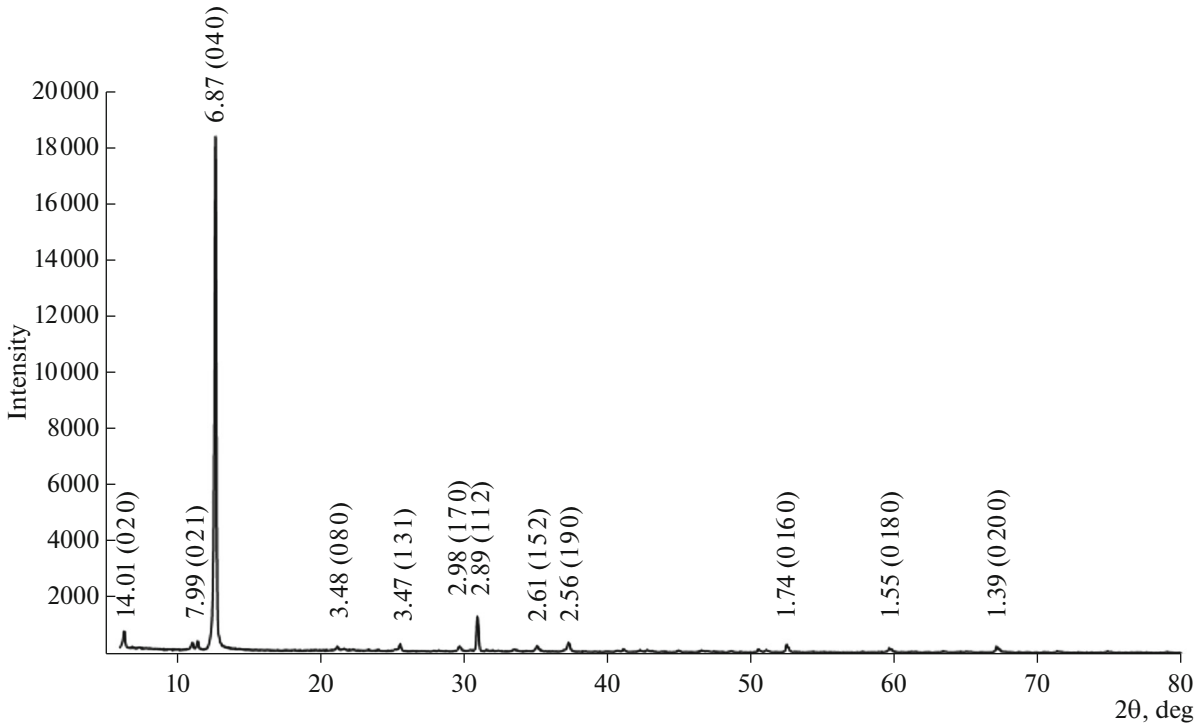

Fig. 1. X-ray diffraction pattern of the bobierrite. Spacing values are in Å.

The following equipment was used in the course of this study: Camebax-microbeam microprobe at the Fersman Mineralogical Museum, Russian Academy of Sciences; STOE STADI MP X-Ray powder diffractometer and FSM-1201 IR Furrier spectrometer, EnSpector R532 Raman microscope, and Setaram Tian–Calvet microcalorimeter at the Geological Faculty of the Moscow State University; and NETZSCH TG 209 F1 thermogravimetric analyzer and NETZSCH DSC 204 F1 differential scanning calorimeter at the Chemical Faculty of the Moscow State University.

RESULTS AND DISCUSSION

Samples

Data of *chemical analysis* of the samples are presented in Table 1. The chemical formulas were normalized to three cations for kovdorskite and five cations for bobierrite and are $Mg_{1.97}Mn_{0.01}[PO_4]_{1.02}(OH)_{0.90} \cdot 2.96H_2O$ and $Mg_{2.97}Fe_{0.02}Mn_{0.01}[PO_4]_{2.00} \cdot 8.20H_2O$, respectively. These formulas are close to the theoretical ones for kovdorskite $Mg_2[PO_4](OH) \cdot 3H_2O$ and bobierrite $Mg_3[PO_4]_2 \cdot 8H_2O$. All thermodynamic constants were calculated in this work for the minerals corresponding to their theoretical formulas.

The *X-ray diffraction spectra* of the natural hydrous phosphates (Figs. 1, 2) are consistent with data on natural samples from the Kovdor Massif in the RRUFF (RRUFF project) international database and correspond to bobierrite and kovdorskite.

The *Raman spectra* of the minerals (Figs. 3b, 4b) are consistent with the spectra of bobierrite in the database RRUFF # R 060681 (RRUFF project) and in (Frost et al., 2002) and the spectra of kovdorskite in RRUFF # R 060579 (RRUFF project) and (Morrison et al., 2012; Frost et al., 2013).

The Raman spectrum of the bobierrite (Fig. 3b) is close to that of vivianite, a hydrous Fe phosphate, $Fe_3[PO_4]_2 \cdot 8H_2O$, which was studied in (Ogorodova et al., 2017). The region of 900–1100 cm^{-1} shows an intense line of totally symmetric valence vibration at 953 cm^{-1} and low-intensity lines of triply degenerate antisymmetric stretching vibrations of the $[PO_4]^{3-}$ ion at 1002, 1075, and 1100 cm^{-1}. The region 400–600 cm^{-1} includes lines pertaining to triply degenerate deforma-

Table 1. Chemical composition of the minerals

Oxide	Kovdorskite	Bobierrite
MgO	36.78	28.84
MnO	0.21	0.24
FeO	–	0.45
P_2O_5	33.62	34.17
H_2O*	28.41	35.87

* Thermogravimetric data.

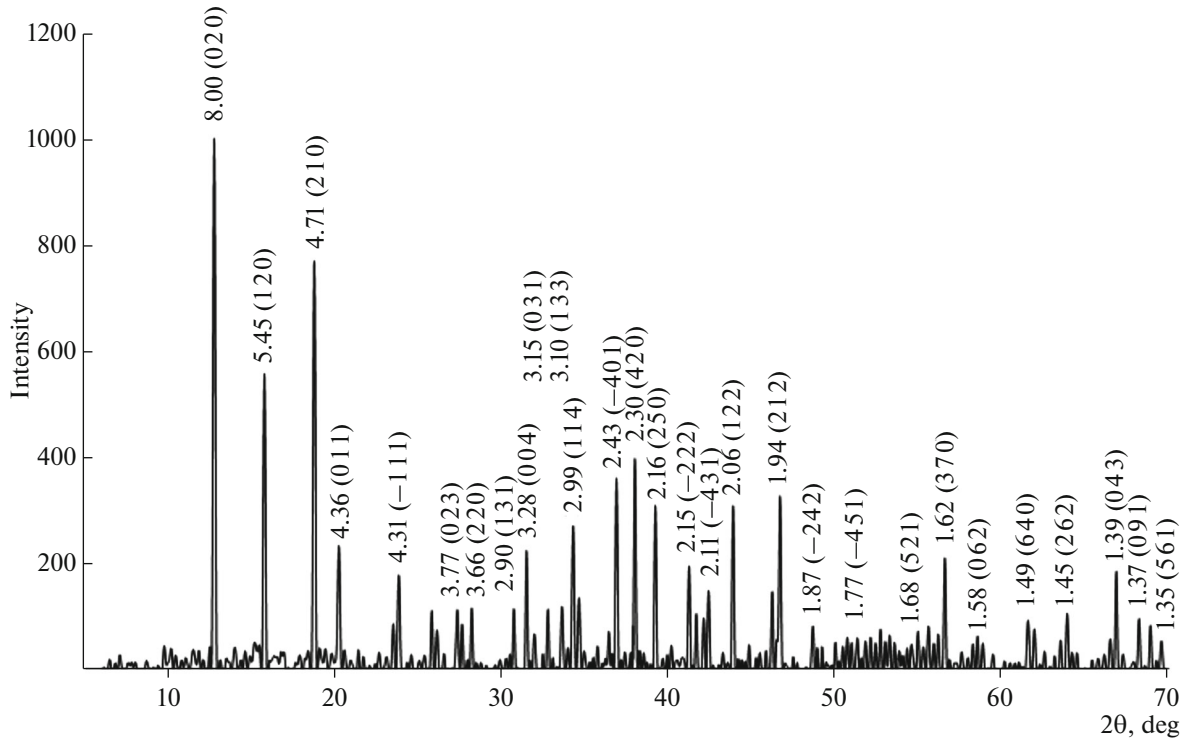

Fig. 2. X-ray diffraction pattern of the kovdorskite. Spacing values are in Å.

tion vibrations (at 558 cm^{-1} and a shoulder at 584 cm^{-1}) and doubly degenerate vibrations of the PO_4 tetrahedron. The frequency region below 400 cm^{-1} includes cation translational vibrations and lattice modes. The high-frequency region shows low-intensity lines corresponding to valence vibrations of the water molecule at 3121, 3208, 3429, and 3439 cm^{-1}. The occurrence of molecular water in the mineral is confirmed by the presence of a scattering line corresponding to the deformation vibrations of the water molecule (1627 cm^{-1}).

The Raman spectrum of the kovdorskite (Fig. 4b) is similar in general configuration to the bobierrite spectrum. The frequency region of 950–1100 cm^{-1} shows an intense line of totally symmetric valence vibrations at 966 cm^{-1} and low-intensity lines of triply degenerate antisymmetric stretching vibrations of the $[PO_4]^{3-}$ ion at 1057 and 1093 cm^{-1}. The region of 400–600 cm^{-1} includes lines corresponding to triply degenerate deformation vibrations (456 and a shoulder at 479 cm^{-1}) and to doubly degenerate deformation vibrations (539 and a shoulder at 576 cm^{-1}) of the PO_4 tetrahedrons. The region below 400 cm^{-1} shows lines of cation translational vibrations and lattice modes. The region of the stretching vibrations of the OH group exhibits low-intensity lines pertaining to the vibrations of the water molecule (at 2986, 3219, and 3383 cm^{-1}). The frequency of 1642 cm^{-1} corresponds to the deformation vibrations of the water molecule. The occurrence of the OH group in the structure of the mineral is reflected in the kovdorskite spectrum as an intense narrow line at 3686 cm^{-1}.

The *IR absorption spectra* of the bobierrite (Fig. 5c) and kovdorskite (Fig. 6f) are consistent with data on samples of these minerals from the Kovdor Massif (Chukanov, 2014): nos. P39 and P107 for the bobierrite and kovdorskite, respectively. Analogous data are presented in (Frost et al., 2002; Morrison et al., 2012; Frost et al., 2013) and in the database RRUFF no. 050505.1 (RRUFF project)

The IR absorption spectrum of the bobierrite (Fig. 5c) is also similar to the IR spectrum of the group-forming mineral vivianite (Ogorodova et al., 2017). The region of the valence vibrations of the OH group shows a broad intense absorption band with one narrow (3474 cm^{-1}) and three smoothed-out components at 3285, 3187, and 3110 cm^{-1}. An intense band corresponding to the deformation vibrations of water molecules shows a maximum at 1594 cm^{-1} and a shoulder at 1660 cm^{-1}. The intense band corresponding to the valence vibrations of the $[PO_4]^{3-}$ ion consists of two components with maxima at approximately 1010 and 1037 cm^{-1} and two shoulders at approximately 976 and 1079 cm^{-1}. The intense lines with maxima at 709 and 855 cm^{-1} correspond to the librational vibrations of the water molecules. The absorption bands at 547 and 574 cm^{-1} and a shoulder at 549 cm^{-1} pertain to triply degenerate deformation vibrations of the PO_4 tetrahedron. The band with a frequency of 474 cm^{-1} corre-

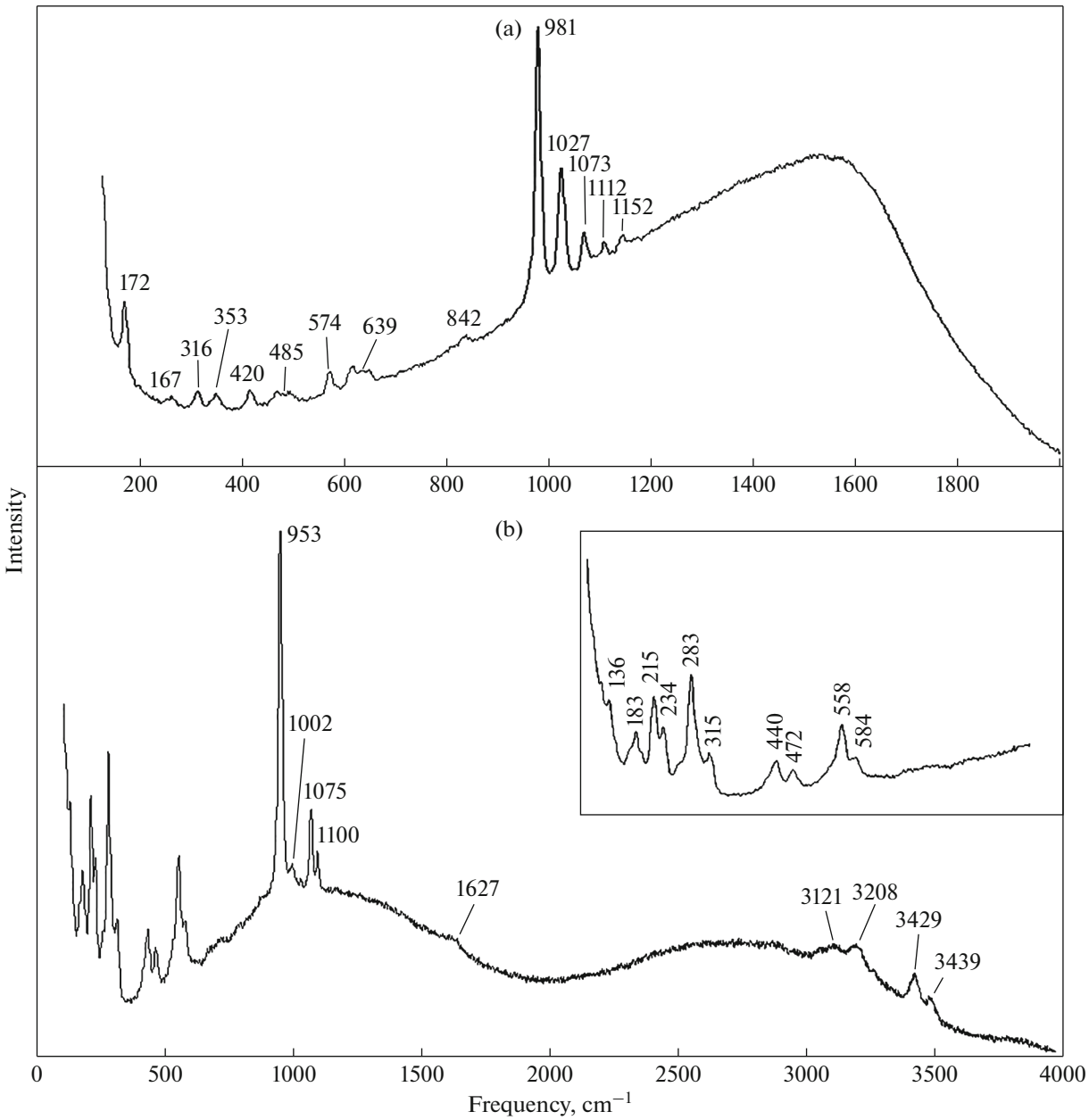

Fig. 3. Raman spectra of (a) products of bobierrite heating to $T = 980$ K and (b) bobierrite itself.

sponds to the doubly degenerate deformation vibration of $[PO_4]^{3-}$.

The high-frequency region of the IR absorption spectrum of the kovdorskite (Fig. 6f) shows an intense broad absorption band of the valence vibrations of molecular water, with two maxima at 3207 and 3402 cm^{-1} and an intense narrow band at 3691 cm^{-1}, which corresponds to the valence vibrations of the OH groups that coordinate the cations. A band of deformation vibrations of the water molecules is registered at about 1658 cm^{-1}. An intense absorption band corresponding to the valence vibrations of the $[PO_4]^{3-}$ ion has a maximum at a frequency of 1037 cm^{-1} and two shoulders at 1018 and 1067 cm^{-1}. The absorption lines at approximately 652 and 782 cm^{-1} and a shoulder at 812 cm^{-1} pertain to the librational vibrations of the hydroxyl groups and water molecules. The low-frequency region shows lines of triply and double degenerate deformation vibrations of the $[PO_4]^{3-}$ ion at 564, 453, and 421 cm^{-1}.

Figures 7 and 8 exhibit the results of *thermal analysis* of the minerals. The TG and DTG curves of the bobierrite (Fig. 7) show that it is dehydrated in two stages. The mineral starts to rapidly lose mass at a tem-

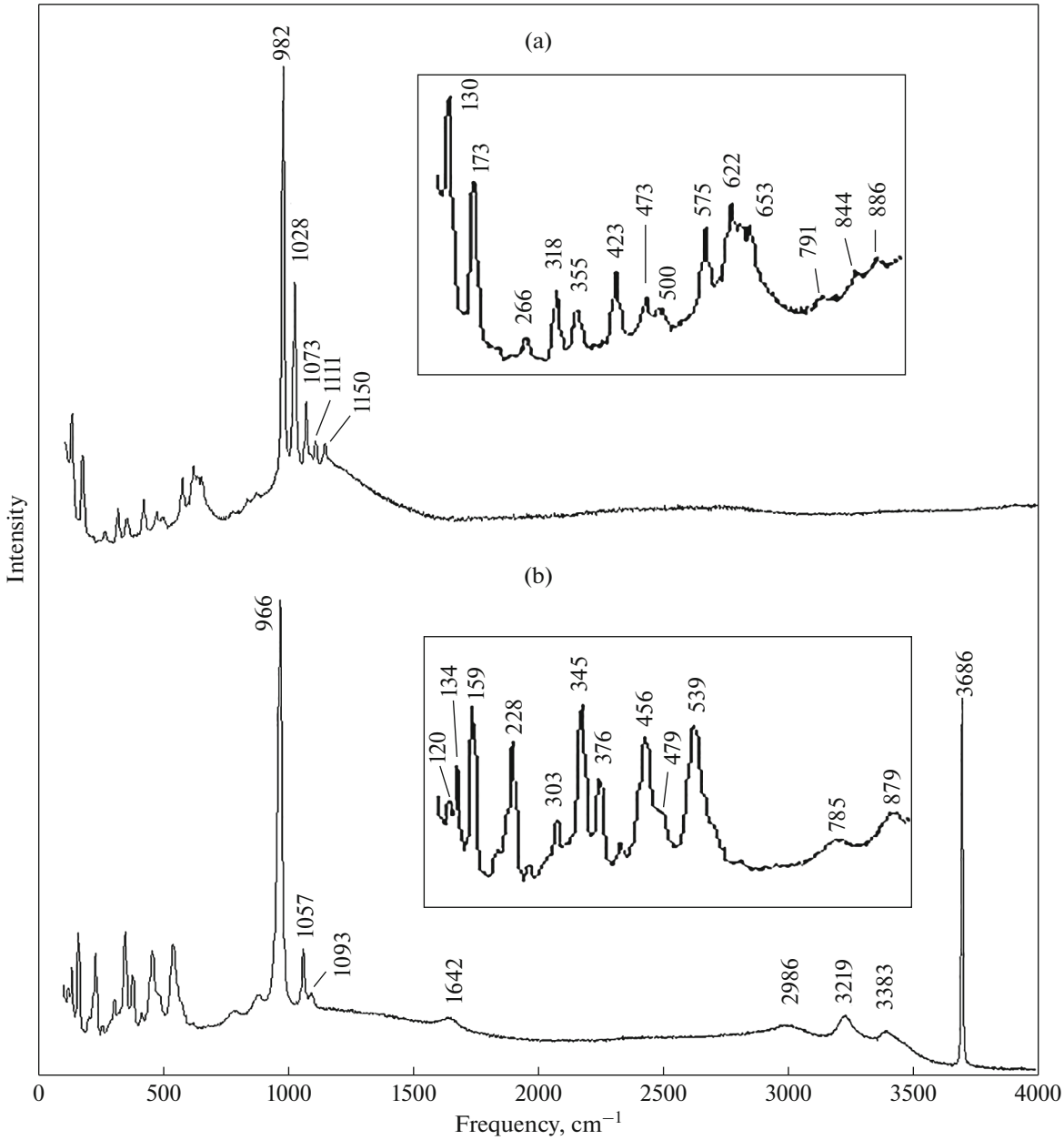

Fig. 4. Raman spectra of products of kovdorskite heating to (a) $T = 1140$ K and (b) kovdorskite itself.

perature close to 340 K, and water removal from it is completed at 980 K. During the first stage at 340–510 K, the mass loss is ~31.2% (about seven water molecules are removed), and the loss during the second stages is ~4.7% (the last remaining water molecule is lost). The IR spectrum of bobierrite heated to 510 K (Fig. 5b) is remarkably modified: the high-temperature region contains no intense band at 3474 cm^{-1}, the overall intensity of the absorption band of the valence vibrations of the water molecule is much lower, as also is the intensity of the absorption band of deformation vibrations at 1642 cm^{-1}, and the spectrum has no absorption bands related to librational vibrations at 709 and 855 cm^{-1}. The absorption bands at 450–590 and 950–1100 cm^{-1}, which correspond to the deformation and valence vibrations of the $[PO_4]^{3-}$ ion in the bobierrite structure, acquire a configuration typical of phosphate glass. The IR absorption spectrum of sample dehydrated at 980 K (Fig. 5a) indicates that a new highly crystalline phase is present: this is farringtonite $Mg_3[PO_4]_2$ (Chukanov and Chervonnyi, 2016; no. P 481). The presence of newly formed farringtonite also follows from the IR spectrum of the sample calcinated at $T = 980$ K (Fig. 3a). This spectrum coincides with data in RRUFF no. R 130127 (RRUFF project) and (O'Neill et al., 2006).

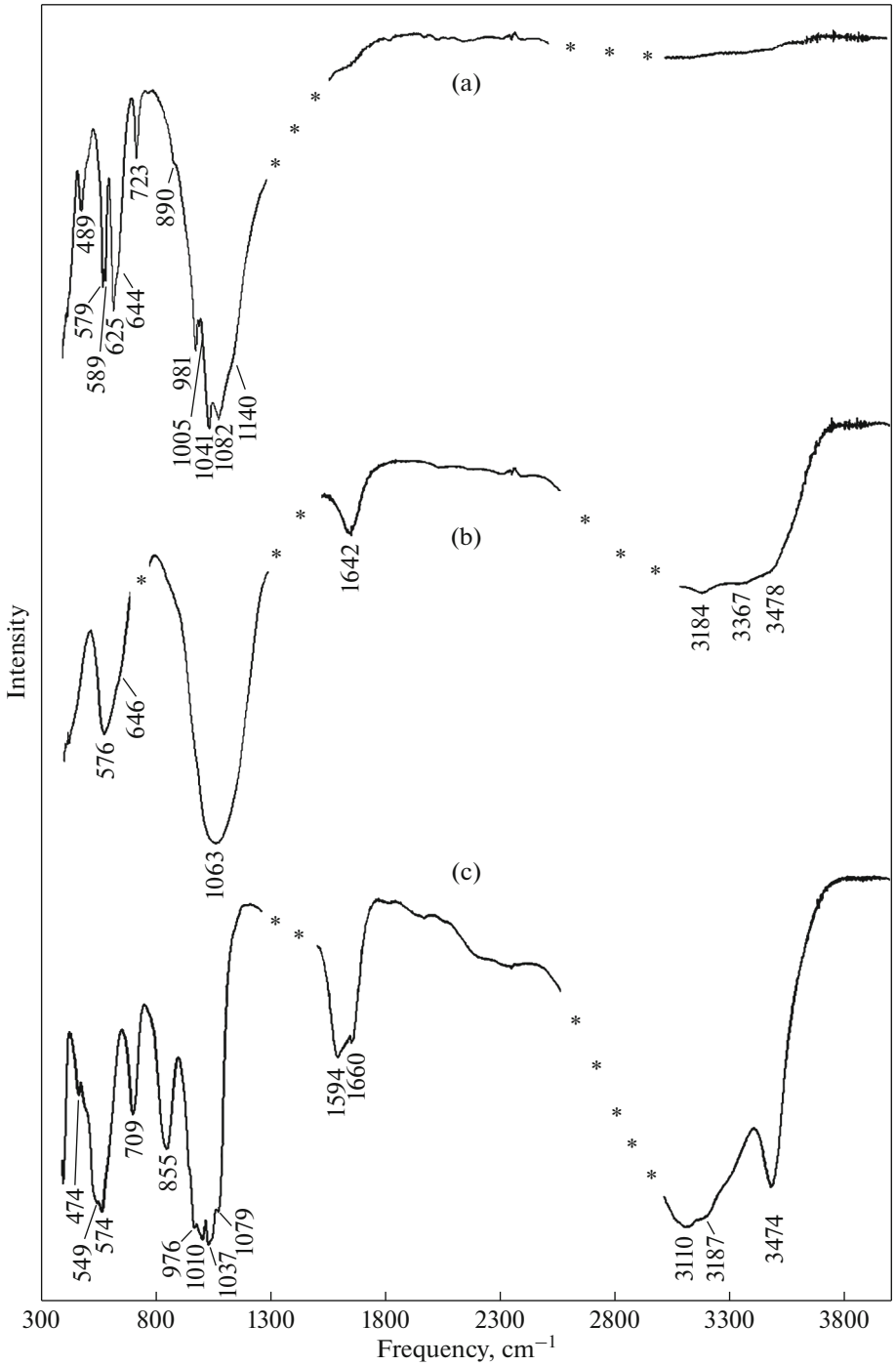

Fig. 5. IR absorption spectra of products of bobierrite heating to (a) $T = 980$ K and (b) 510 K, and (c) bobierrite itself.

The TG and DTG curves of the kovdorskite (Fig. 8) show four mass–loss stages: (1) at 465–550 K, which corresponds to ~15.8% loss of the sample mass (removal of ~2% water molecules), (2) 550–730 K (mass loss of ~4.6%), (3) 730–810 K (~further ~4.1% mass loss), and (4) 810–1140 K (loss of the remaining water, ~3.8%). To elucidate in greater detail the sequence of water removal from kovdorskite, we have studied the IR spectra of products obtained at various heating stages of this mineral. The IR spectra of kovdorskite heated to 550 K (point *A* on the TG curve, Fig. 8) shows a decrease in absorbance intensity only in the regions of deformation and valence vibrations of water. The spectrum (Fig. 6d) of the sample heated to 730 K (Fig. 8, point *B*) provides evidence of the total dehydroxylation of the mineral (the absence of an intense band at 3693 cm^{-1} correspond to absorption by hydroxyl groups), further dehydration of the sample,

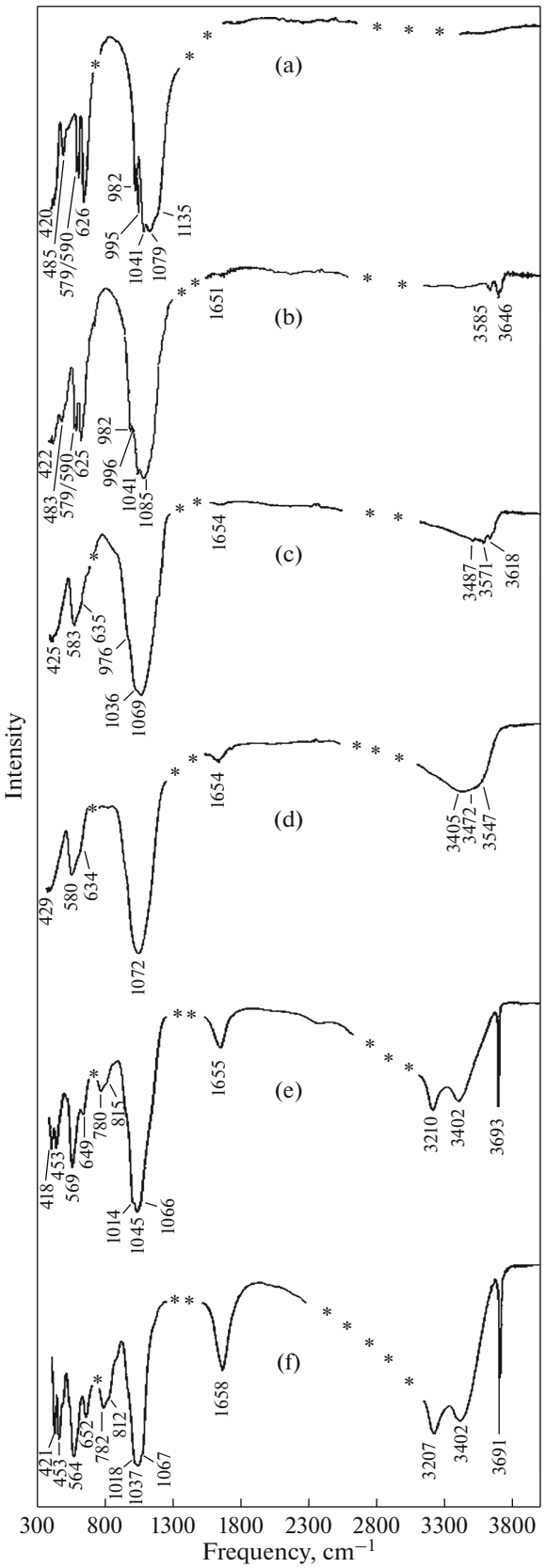

Fig. 6. IR absorption spectra of products of kovdorskite heating to (a) $T = 1140$, (b) 980, (c) 810, (d) 730, (e) 550 K, and (f) kovdorskite itself.

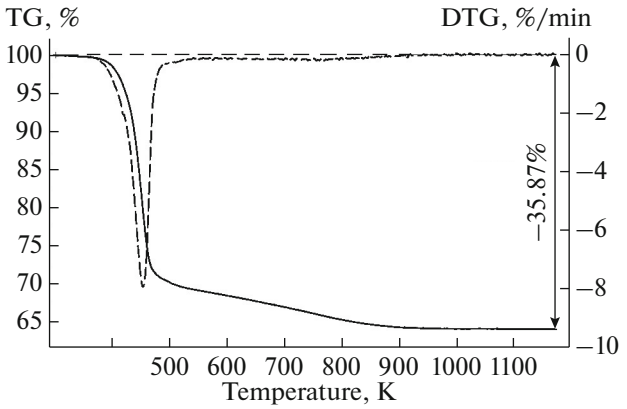

Fig. 7. TG and DTG curves of bobierrite heating.

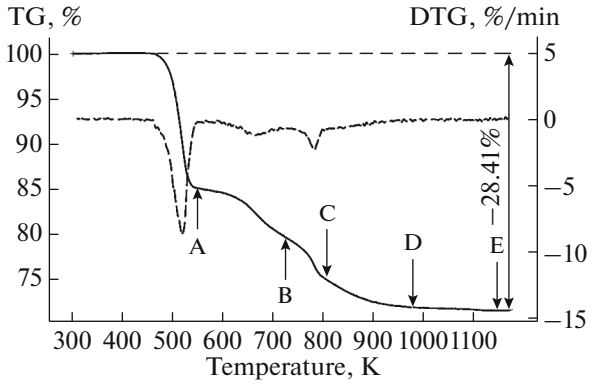

Fig. 8. TG and DTG curves of kovdorskite heating.

and the development of a glass-like phase. The IR spectrum (Fig. 6c) of the product of heating to 810 K (Fig. 8, point *C*) shows that the glass-like phase with a low water concentration is preserved. The spectrum (Fig. 6b) of the sample heated to 980 K (Fig. 8, point *D*) provides evidence of farringtonite $Mg_3[PO_4]_2$ crystallization and the preservation of the remaining water. The further heating of the sample to $T = 1140$ K (Fig. 8, point *E*) leads to the complete dehydration of the farringtonite (Fig. 6a), which exactly agrees with the results of IR spectroscopy (Fig. 4a). The heating of the kovdorskite to $T = 550$ K thus leads to the removal of its crystal-hydrate water and part of its OH groups, and heating to 730 K results in the complete dehydroxylation of the mineral and its further dehydration with the formation of phosphate glass. The further heating to 1140 K is associated with the crystallization of anhydrous Mg phosphate.

Enthalpy of Formation

The average values of seven Tian–Calvet calorimetric measurements of $[H^0(973\text{ K}) - H^0(298.15\text{ K}) + \Delta_{\text{dissol.}}H^0(973\text{ K})]$ were 1956.7 ± 37.9 J/g = 420.0 ± 8.1 kJ/mol (M = 214.64 g/mol) for kovdorskite

and 2078.3 ± 22.5 J/g = 845.8 ± 9.1 kJ/mol (M = 406.98 g/mol) for bobierrite (the inaccuracies are calculated at 95% probability).

The data thus acquired were used to calculate the standard enthalpy of formation of the hydrous magnesium phosphates, using reactions (1) and (2) and Eqs. (3) and (4)

$$2MgO + 0.5P_2O_5 + 7/3Al(OH)_3 = Mg_2[PO_4](OH) \cdot 3H_2O\ (\text{kovdorskite}) + 7/6Al_2O_3, \quad (1)$$

$$3MgO + P_2O_5 + 16/3Al(OH)_3 = Mg_3[PO_4]_2 \cdot 8H_2O(\text{bobierrite}) + 8/3Al_2O_3, \quad (2)$$

$$\Delta_{r(1)}H^0(298.15\,K) = \Sigma\nu_i\Delta H\text{oxi}_i - \Delta H\text{mineral}, \quad (3)$$

$$\Delta_f H^0_{el}(298.15\,K)\text{mineral} = \Delta_{r(1,2)}H^0(298.15\,K) + \Sigma\nu_i\Delta_f H^0_{el}(298.15\,K)\text{oxi}_i, \quad (4)$$

where $\Delta H = [H^0(973\,K) - H^0(298.15\,K) + \Delta_{dissol.}H^0(973\,K)]$ is calorimetric data on the minerals, MgO, P_2O_5, Al_2O_3, and $Al(OH)_3$ (Table 2); the required values of $\Delta_f H^0_{el}(298.15\ K)$ of the latter are reported in the same table. The calculated enthalpies of formation of kovdorskite and bobierrite are given in Table 3.

Enthalpy of Dehydration

Data obtained by studying water removal from kovdorskite and bobierrite using differential scanning calorimetry are presented in Figs. 9 and 10. The heat corresponding to the first dehydration stage and reflected in the DSC curve of bobierrite (Fig. 9) is Q = 1097 J/g = 447 kJ/mol. The DSC curve for kovdorskite (Fig. 10) shows three endothermic effects related to water removal from the mineral. The measured heat values correspond to the stepwise mass loss were Q_1 = 443 J/g = 95 kJ/mol (removal of the crystal-hydrate water and partly OH groups); Q_2 = 194 J/g = 42 kJ/mol (removal of the crystal-hydrate water and remaining OH groups); Q_3 = 49 J/g = 11 kJ/mol (loss of crystal-hydrate water).

Gibbs Energy of Formation

To calculate the Gibbs energy of formation of the hydrous phosphates from elements, we have evaluated the standard entropy values not available from the literature (Table 3). The calculations were carried out according to Latimer's method, with regard for the average entropy values for cations and anions in the solid compounds and the entropy contribution of the crystal-hydrate water (Naumov et al., 1971). The estimates of $S^o(298.15\ K)$ and the enthalpies of formation determined in the course of this research were used to calculate $\Delta_f G^0_{el}(298.15\ K)$ for bobierrite and kovdorskite (Table 3). The Gibbs energy value thus obtained (−5472 ± 16 kJ/mol) are close to the value determined in studying exchange reactions in (Duff, 1971) and reported without error (−5450.5 kJ/mol).

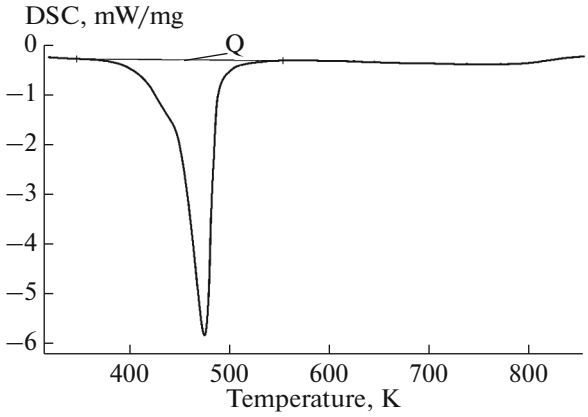

Fig. 9. DSC curve of bobierrite.

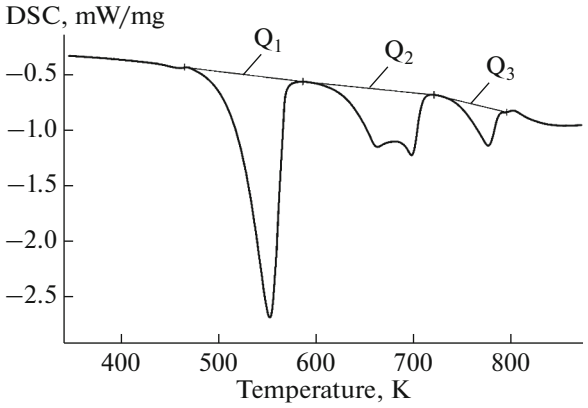

Fig. 10. DSC curve of kovdorskite.

Table 2. Thermochemical data used to calculate the enthalpies (kJ/mol) of formation of the hydrous magnesium phosphates

Component	ΔH[a]	$-\Delta_f H^0_{el}$ (298.15 K)[b]
MgO(periclase)	36.38 ± 0.59[c]	601.6 ± 0.3
Al_2O_3(corundum)	107.38 ± 0.59[d]	1675.7 ± 1.3
P_2O_5(c)	−326.48 ± 1.21[e]	1504.9 ± 0.5
$Al(OH)_3$(gibbsite)	172.6 ± 1.9[f]	1293.1 ± 1.2

[a]$\Delta H = [H^0(973\ K) - H^0(298.15\ K) + \Delta_{dissol}H^0(973\ K)]$. [b]Tabulated data from (Robie and Hemingway, 1995). [c, d]Calculated using tabulated data on $[H^0(973\ K) - H^0(298.15\ K)]$ (Robie and Hemingway, 1995) and experimental data on dissolution $\Delta_{dissol}H^0(973\ K)$: [c](Navrotsky and Coons, 1976), [d](Ogorodova et al., 2003). [e]Based on data from (Ushakov et al., 2001). [f]Based on data from (Ogorodova et al., 2011).

Table 3. Thermodynamic properties of bobierrite and kovdorskite: our data (this publication)

Formula of mineral	$-\Delta_f H^0_{el}$(298.15 K), kJ/mol	S^0(298.15 K)*, J/(K mol)	$-\Delta_f G^0_{el}$(298.15 K), kJ/mol
$Mg_3[PO_4]_2 \cdot 8H_2O$ bobierrite	6167 ± 16	535.6	5472 ± 16
$Mg_2[PO_4](OH) \cdot 3H_2O$ kovdorskite	3251 ± 10	263.6	2917 ± 10

CONCLUSIONS

Chemical analyses of Martian meteorites found on the Earth and data of Martian surface scanning by the Spirit and Opportunity Mars exploration rovers of NASA have shown that phosphorus content in the Martian lithosphere is roughly one order of magnitude higher than the average concentration of this element in terrestrial rocks (Dreibus et al., 1996; Wänke and Dreibus, 1998). Ample evidence indicates that hydrous phosphates are currently present on Mars and that the surface of this planet contained water in the historical past. The thermodynamic parameters we obtained for kovdorskite and bobierrite can be recommended to use in simulating mineral-forming processes in the Martial lithosphere.

In the Earth's lithosphere, bobierrite occurs much more widely than kovdorskite and is formed in a great diversity of geological environments: in dolomite veins hosted in apatite ores and phoscorites (as in the iron ore quarry at the Kovdor deposit, Russia; Liferovich et al., 1999), as an alteration product of primary phosphate minerals in granite pegmatites in Bendata, Portugal (Garate-Olabe et al., 2012) and in Wodgina, Australia (Mason and Dunn, 1974); and in phosphorus-rich sedimentary iron ores in Kerch, Crimea, Russia. Fine-grained crusts of this mineral are produced by chemical alterations in guano at Mejillones, Chile (Atencio et al., 2012) and in elephant teeth at Edgerton, Minnesota, United States (Gruner and Stauffer, 1943). Kovdorskite is endemic to the Kovdoir Massif, although this mineral was found at the deposit as fairly large spectacular crystals and crystal aggregates up to 10 cm (Liferovich et al., 1999). The thermodynamic characteristics of kovdorskite and bobierrite reported in this publication can be used to constrain the stability fields of minerals and to elucidate the reasons for their highly uneven distribution in the Earth's lithosphere.

FUNDING

This study was supported by the Russian Foundation for Basic Research, project no. mk-18-29-12128.

REFERENCES

D. Atencio, N. V. Chukanov, F. Nestola, T. Witzke, J. M. Coutinho, A. E. Zadov, and G. Färber, "Mejillonesite, a new acid sodium, magnesium phosphate mineral, from Mejillones, Antofagasta, Chile," Am. Mineral. **97**, 19–25 (2012).

N. V. Chukanov, *Infrared Spectra of Mineral Species: Extended Library* (Springer-Verlag GmbH, Dordrecht–Heidelberg–New York–London, 2014).

N. V. Chukanov and A. D. Chervonnyi, *Infrared Spectroscopy of Minerals and Related Compounds* (Springer Cham, Heidelberg–New York–Dordrecht–London, 2016).

G. Dreibus, T. Jagoutz, B. Spettel, and H. Wänke, "Phosphate-mobilization on Mars? Implications from leach experiments on SNCs," Lunar Planet. Sci. Conf. **27**, 323 (1996)

E. J. Duff, "Orthophosphates. Part VIII. The transformation of newberryite into bobierrite in aqueous alkaline solutions," J. Chem. Soc. **A**, 2736–2740 (1971).

M. D. Dyar, E. R. Jawin, E. Breves, G. Marchand, M. Nelms, M. D. Lane, S. A. Mertzman, D. L. Bish, and J. L. Bishop, "Mössbauer parameters of iron in phosphate minerals: Implications for interpretation of martian data," Am. Mineral. **99**, 914–942 (2014).

A. W. Frazier, J. R. Lehr, and J. P. Smith, 'The magnesium phosphates hannayite, schertelite and bobierrite," Am. Mineral. **48**, 635–641 (1963).

R. L. Frost, W. Martens, P. A. Williams, and J. T. Kloprogge, "Raman and infrared spectroscopic study of the vivianite-group phosphates vivianite, baricite and bobierrite," Mineral. Mag. **66** (6), 1063–1073 (2002).

R. L. Frost, A. López, Y. Xi, A. Granja, R. Scholz, and R. M. F. Lima, "Vibrational spectroscopy of the phosphate mineral kovdorskite—$Mg_2(PO_4)(OH) \cdot 3H_2O$," Spectrochim. Acta Part. *A* **114**, 309–315 (2013).

I. Garate-Olabe, E. Roda-Robles, P.-P. Gil-Crespo, A. Pesquera-Pérez, R. Vieira, and A. Lima, "Estudio textural y mineralogico del Dique de Cuarzo con Fosfatos de Folgosinho (Guarda, Portugal)," Macle junio revista de la sociedad espanola de mineralogia **16**, 220–221 (2012).

J. W. Gruner and C. R. Stauffer, "A unique occurrence of bobierrite, $Mg_3(PO_4)_2 \cdot 8H_2O$," Am. Mineral. **28,** 339–340 (1943).

T. Kanazawa, T. Umegaki, and M. Shimizu, "The synthesis of $Mg_3(PO_4)_2 \cdot 8H_2O$ and its new polymorphism," Bull. Chem. Soc. Jpn. **52**, 3713–3717 (1979).

Yu. L. Kapustin, A. V. Bykova, and Z. V. Pudovkina, "Kovdorskite–a new mineral," Zap, Ross. Mineral. O-va, No, 3, 341–347 (1980).

I. A. Kiseleva and L. P. Ogorodova, "An application of high-temperature dissolution calorimetry for determination of enthalpies of formation of hydroxyl-bearing minerals by the example of talc and tremolite," Geokhimiya, No. 12, 1745–1755 (1983).

A. La Iglesia, "Estimating the thermodynamic properties of phosphate minerals at high and low temperature from the sum of constituent units," Estud. Geológ. **65** (2), 109–119 (2009).

R. P. Liferovich, Ya. A. Pakhomovsky, V. N. Ykovenchuk, A. N. Bogdanova, and A. Yu. Bakhchisaraitsev, "Vivianite and bobierrite group minerls from the Kovdor massif," Zap. Ross. Mineral. O-va, No. 6, 109–117 (1999).

R. L. Manly, "The differential thermal analysis of certain phosphates," Am. Mineral. **35**, 108–115 (1950).

B. Mason and P. J. Dunn, "An unusual occurrence of bobierrite at Wodgina, Western Australia," Miner. Record. No. **5**, 265–267 (1974).

S. M. Morrison, R. T. Downs, and H. Yang, "Redetermination of kovdorskite, $Mg_2(PO_4)(OH) \cdot 3H_2O$," Acta Crystallogr. Sect. E **68**, i12–i13 (2012).

G. B. Naumov, B. N. Ryzhenko, and I. L. Khodakovsky, *A Handbook of Thermodynamic Data (for Geologists)* (Atomizdat, Moscow, 1971) [in Russian].

A. Navrotsky and W. J. Coons, "Thermochemistry of some pyroxenes and related compounds," Geochim. Cosmochim. Acta **40**, 1281–1295 (1976).

A. E. O'Neill, D. Uy, and M. Jagner, "Characterization of phosphates found in vehicle-aged exhaust gas catalysts: a Raman study," *SAE* Paper # 2006-01-0410 (2006).

L. P. Ogorodova, L. V. Melchakova, I. A. Kiseleva, and I. A. Belitsky, "Thermochemical study of natural pollucite," Thermochim. Acta **403**, 251–256 (2003).

L. P. Ogorodova, I. A. Kiseleva, L. V. Mel'chakova, M. F. Vigasina, and E. M. Spiridonov, "Calorimetric determination of the enthalpy of formation for pyrophyllite," Russ. J. Phys. Chem. **A85** (9), 1492–1494 (2011).

L. Ogorodova, M. Vigasina, L. Mel'chakova, V. Rusakov, D. Kosova, D. Ksenofontov, and I. Bryzgalov, "Enthalpy of formation of natural hydrous iron phosohate: vivianite," J. Chem. Thermodyn. **110**, 193–200 (2017).

V. E. Ovchinnikov, L. P. Solov'eva, Z. V. Pudovkina, Yu. L. Kapustin, and N. V. Belov, "Crystalline structure of kovdorskite $Mg_2(PO_4)(OH) \cdot 3H_2O$," Dokl. Akad Nauk SSSR **255** (2), 351–354 (1980).

E. V. Ponomareva and N. I. Krasnova, "New data on kovdorskite—$Mg_2(PO_4)(OH) \cdot 3H_2O$," Zap. Vsesoyuz. Mineral. O-va, No. **6**, 92–100 (1990).

R. A. Robie and B. S. Hemingway, "Thermodynamic properties of minerals and related substances at 298.15 K and 1 bar (105 Pascals) pressure and at higher temperatures," U.S. Geol. Surv. Bull. No. 2131, (1995). RRUFF Project. Database of Raman Spectroscopy, X-ray Diffraction and Chemistry of Minerals, http://www.rruff.info/

S. Takagi, M. Mathew, and W. E. Brown, "Crystal structures of bobierrite and synthetic $Mg_3(PO_4)_2 \cdot 8H_2O$," Am. Mineral. **71**, 1229–1233 (1986).

S. V. Ushakov, K. V. Helean, A. Navronsky, and L. A. Boatner, "Thermochemistry of rare-earth orthophosphates," J. Mater. Res. **16** (9), 2623–2633 (2001).

P. Viellard and Y. Tardy, "Thermochemical properties of phosphates, *Phosphate Minerals,* Ed. by J. O. Nriagu, and P. B. Moore (Springer-Verlag, Berlin, 1984), pp. 171–198.

H. Wänke and G. Dreibus, "Chemical composition and accretion history of terrestrial planets," Philos. Trans. R. Sos. London Ser. A **325**, 545–557 (1998).

Translated by E. Kurdyukov